Neuron, Volume *90*

Supplemental Information

Orbitofrontal Cortex Value Signals Depend on Fixation Location during Free Viewing

Vincent B. McGinty, Antonio Rangel, and William T. Newsome

SUPPLEMENTAL FIGURES

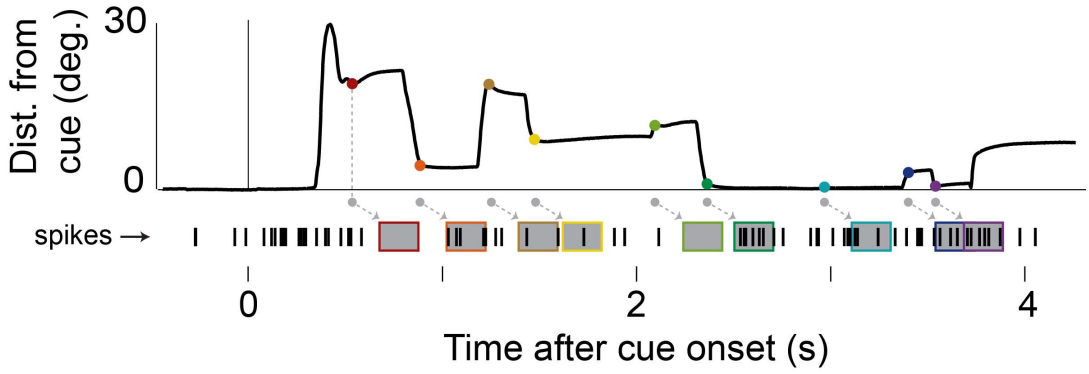

FIGURE S1, related to Figure 3: Extracting fixation-evoked firing from eye position and spiking data: Eye position and neural data in a single trial: the thick black line gives the distance of gaze from the cue, and the raster with black tick marks (below x-axis) shows the spikes of an identified single unit. This is the same data as in Figure 3A. Fixations were detected on the basis of eye velocity (Kimmel et al. 2012). The onset time of each fixation in this trial is marked with a colored dot on the eye trace, and with a corresponding gray dot below the trace. (Note that fixations outside of the 0.50-3.75s eligibility window were not analyzed (Experimental Procedures), and therefore are not marked.) The firing associated with each fixation was calculated as follows: For each fixation, we measured the spike count in a 200ms window that was offset from the beginning of the fixation by a fixed lag. The windows for each fixation are indicated by gray rectangles, with colored borders that correspond to the dots on the eye trace. The lag was determined individually for each neuron based on its activity, as described in the Experimental Procedures; the lag in this example is 140ms, and the median lag across all neurons was 160ms.

Saccades sometimes occurred during the 200ms windows over which spiking was measured (e.g. during the light green window at ~2.3s above). To determine whether this ongoing saccadic activity could contribute to variability in fixation-evoked responses, we asked whether peri-saccadic firing exhibited classical encoding of saccadic vectors (particular combinations of direction and amplitude, (Bruce and Goldberg, 1985)) using a factorial ANOVA. Fewer than 1% of neurons had peri-saccadic encoding of saccade vectors (significant effect at $p<0.05$, corrected), indicating that ongoing saccadic behavior contributed negligibly to the fixation-evoked response.

In rare instances, two firing windows overlapped with one another (e.g. the last two fixations above), so that a single spike could be counted as being evoked by both fixations. However, fewer than 4% of fixations had the potential to produce twice-counted spikes, due to the sparse firing of many neurons and to the 100ms minimum fixation dwell time that we imposed on the data. Separate analyses that excluded these fixations yielded results that were not different from those shown here (not shown).

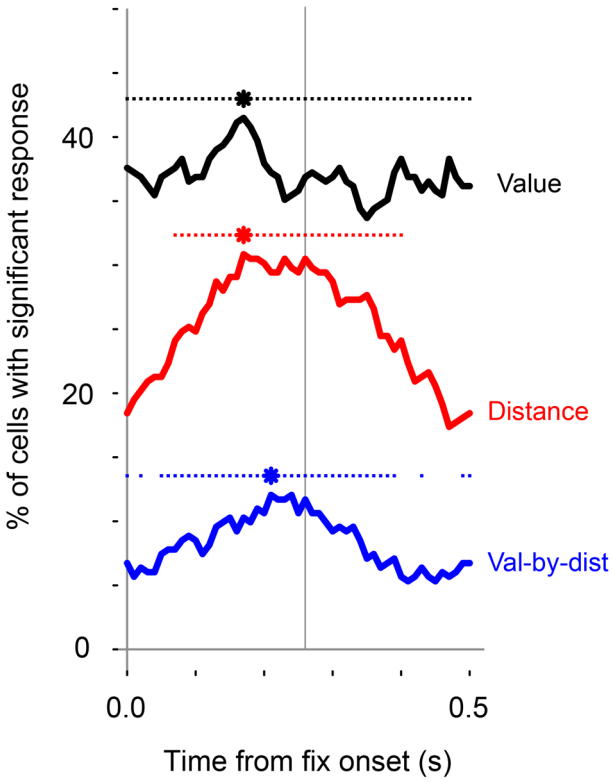

FIGURE S2, related to Figure 5: Time course of value and gaze distance encoding relative to fixation onset: The GLM given by Equation 1 was fit to firing time-locked to fixation onset, using 200ms windows moved in 10ms increments, with window centers ranging from 0 to 500ms relative to fixation onset. For each window, we found the percentage of cells with significant effects ($p<0.05$, corrected within time point, by Holm's method), and these percentages are plotted in the solid black, red, and blue lines. Each asterisk shows the time of the peak percentage for a given variable, and the adjacent dotted lines show times points where the percentages are *not different* from peak levels, by a chi-squared test for proportions (p *greater than* 0.05 after correction within variable, by Holm's method). The gray vertical line shows the center of the typical window used in the main analysis (results in Figures 2-5); this was found by taking the median of all the cell-specific post-fixation windows, which were calculated as described in Experimental Procedures.

For the distance and interaction term variables (red and blue) the maximum percentage occurs approximately 0.2ms after fixation onset, and falls below peak levels in earlier and later time windows (near 0 and 0.5s). The peak at 0.2s is consistent with the typical visual response latency of OFC neurons. The below-peak percentages in the early and late windows is consistent with the fact that gaze distance is changing constantly throughout a trial, meaning that the firing in these time windows reflects the (uncontrolled) gaze distance of fixations occurring before and after the reference fixation. In contrast, encoding of the value variable does not significantly differ from peak levels across the time windows tested. This is expected due to the structure of the task and of the model: within a trial, cue value is constant (unlike gaze distance), and using the GLM it is possible to extract the contribution that value makes to firing *independent* of the contribution of gaze distance, whose effect on firing is captured by the other two regressors.

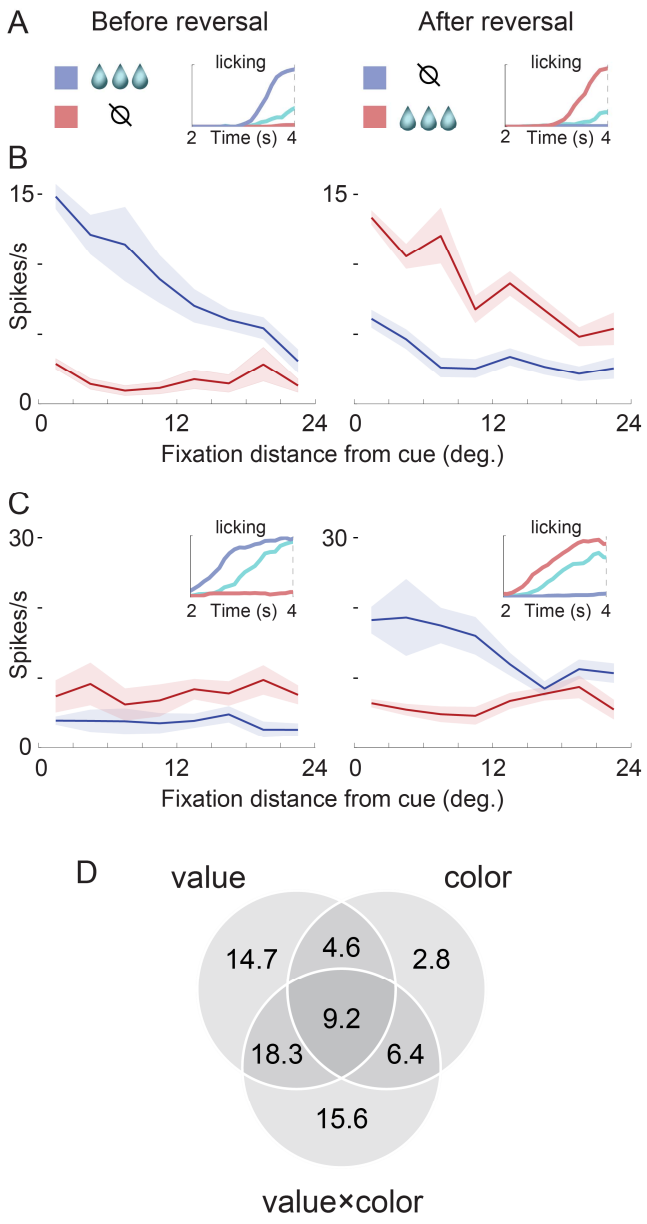

FIGURE S3, related to Figure 5: Color-value reversal test: (A) Reversal of color-reward associations, and the licking responses before and after reversal. (B) Fixation-evoked firing of an identified single unit as a function of fixation location, before and after reversal (same session as in A). Firing for small reward cue is omitted for clarity. (C) A second example of single unit firing before (left) and after reversal (right), with licking responses shown in the inset. (D) Percent of neurons (n = 109 tested) with firing significantly modulated ($p<0.05$ corrected) by cue value, cue color, and the value-by-color interaction, as determined by a GLM. 46.8% of cells were significantly modulated by cue value, 49.5% by the value-by-color interaction, and 22.9% by cue color.

A

% of neurons with effects at p<0.05	Variables of interest			Oculomtor co-regressors		
	value	distance	value-by-dist	saccade ampl.	saccade velocity	dwell time
uncorrected	59.4	48.8	27.9	17.3	12.7	19.8
corrected	35.0	28.6	9.2	2.1	0.7	3.9

B

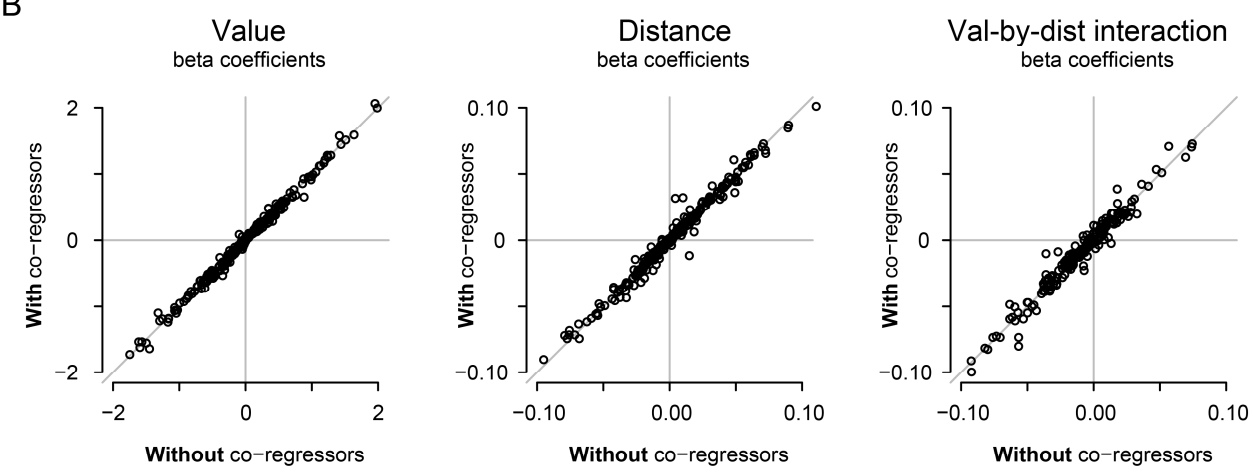

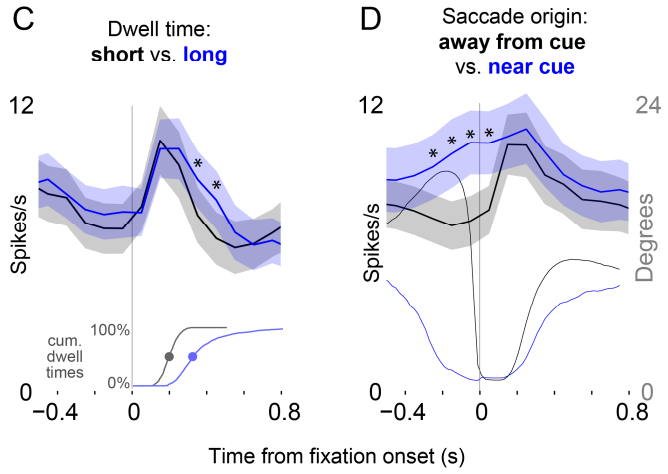

FIGURE S4, related to Table 1: Effects of other oculomotor variables: (A) Percent of neurons with significant effects in a GLM that was similar to the one given by Equation 1, but included three co-regressors that describe oculomotor variables *other* than fixation distance. Including the co-regressors does not substantially change the results for the variables of interest (compare to Table 1). (B) In each plot, the x-axis shows the beta coefficients resulting from the GLM without oculomotor co-regressors (Equation 1, same data as in Figure 5), and the y-axis shows the coefficients obtained with these co-regressors included in the model. All correlations are above $r = 0.98$. (C,

D) To confirm the GLM results in A, in a separate analysis we considered a subset of the data that isolates *excitatory* responses evoked by fixations on or near the cues, and that also holds cue value constant (see Supplemental Experimental Procedures). The PSTHs here show the responses evoked by these on-cue fixations, averaged across cells (mean and SEM). The stars indicate a significant difference between the blue and black curves ($p<0.05$ uncorrected, by Wilcoxon rank sum test). In Panel C, fixations for each cell were median split according to the dwell time of the fixation. Note the overall similar response regardless of dwell time. The thin lines below show the cumulative dwell times across all fixations used in this graph; dots indicate medians. 59 neurons contributed to this analysis. In Panel D, fixations within each cell were divided according to whether the prior fixation was near or away from the cue, effectively dividing them according to the amplitude of the prior saccade. Note the similar response after t = 0, indicating that saccade amplitude did not modulate the response. The large difference in firing prior to t=0 reflects the fact that the fixation immediately prior to t=0 was on or near the cue for the blue data, but was away from the cue for the black data. The thin lines show the eye position relative to the cue, averaged across all fixations within a given condition (right y-axis scale). 69 neurons contributed to this analysis.

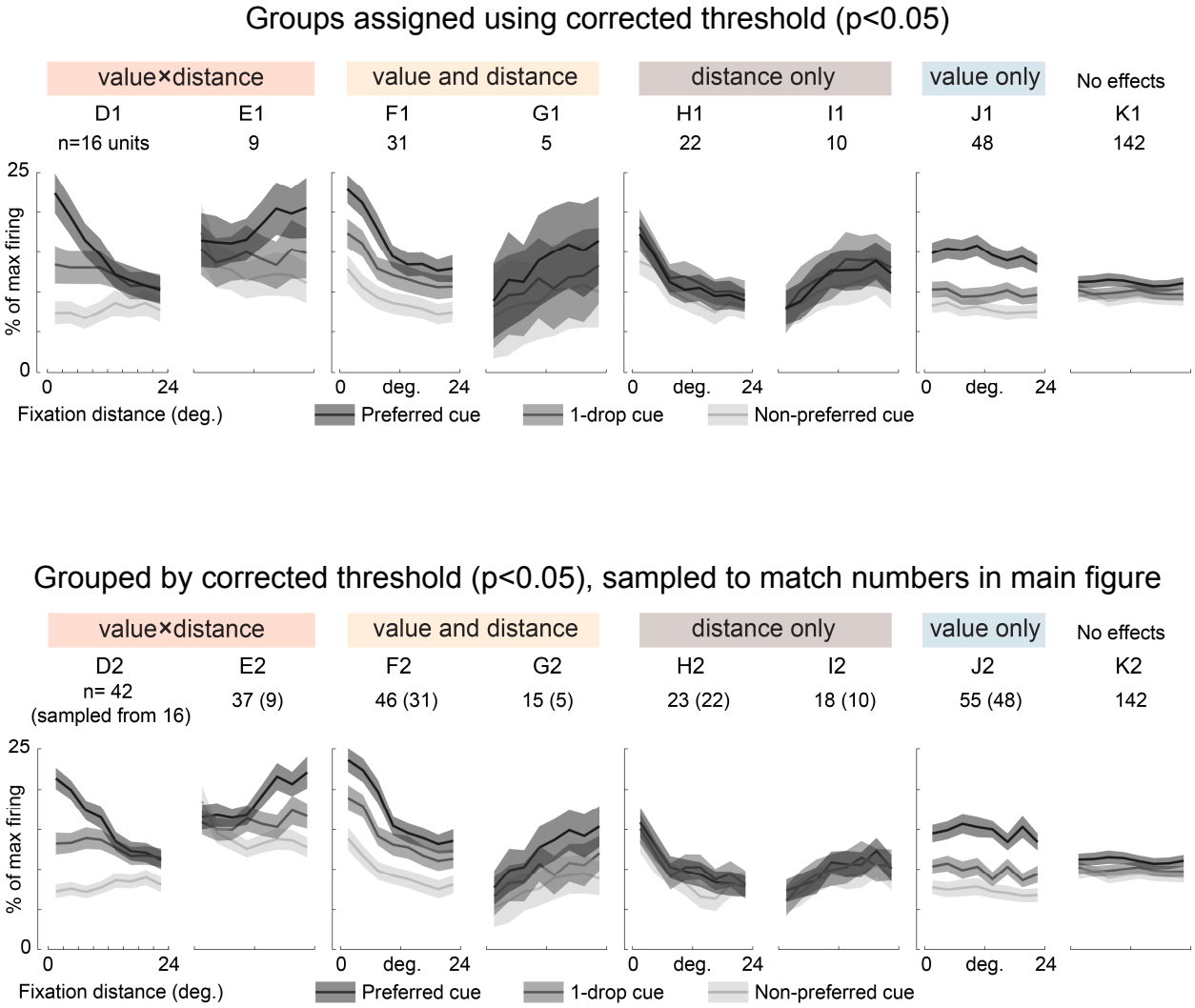

FIGURE S5, related to Figure 5, population firing using cells grouped according to a corrected threshold. In panels D1-K1, the conventions and data are the same as in Figure 5D-K, except that cells are sorted into groups according to the corrected significance threshold, corresponding to the percentages shown in parentheses in Figure 5A. The firing patterns here are very similar to those in the main figure. However, two features bear notice: First, the individual cells in panel K1 are classified as having “no effect”, but as a group they show what appears to be stratification of firing according to cue value. This suggests that one or more cells with nontrivial value effects are misclassified here (due to the use of a corrected threshold), ultimately masking these important population-level effects. To minimize this kind of misclassification and masking of responses, we use an uncorrected threshold in the main figure (Figure 5D-K).

Second, the error bars (shaded regions) are larger in D1-K1 than in the main figure, which could be due to either the reduced number of cells contributing to the graphs (numbers above the graphs) or to the response variability among those cells that do contribute. To determine the effects of cell number here, in panels D2-K2 we re-plot the data in a way that preserves the overall response patterns of panels D1-K1, yet adjusts for the reduced number of neurons. This was done by drawing samples, with replacement, from the cells used in panels D1-K1, until the cell numbers matched those in the main figure. Qualitatively, the error bar sizes in D2-K2 are very similar to those in the main figure, suggesting that the larger error bars in D1-K1 are largely due to the reduced cell number.

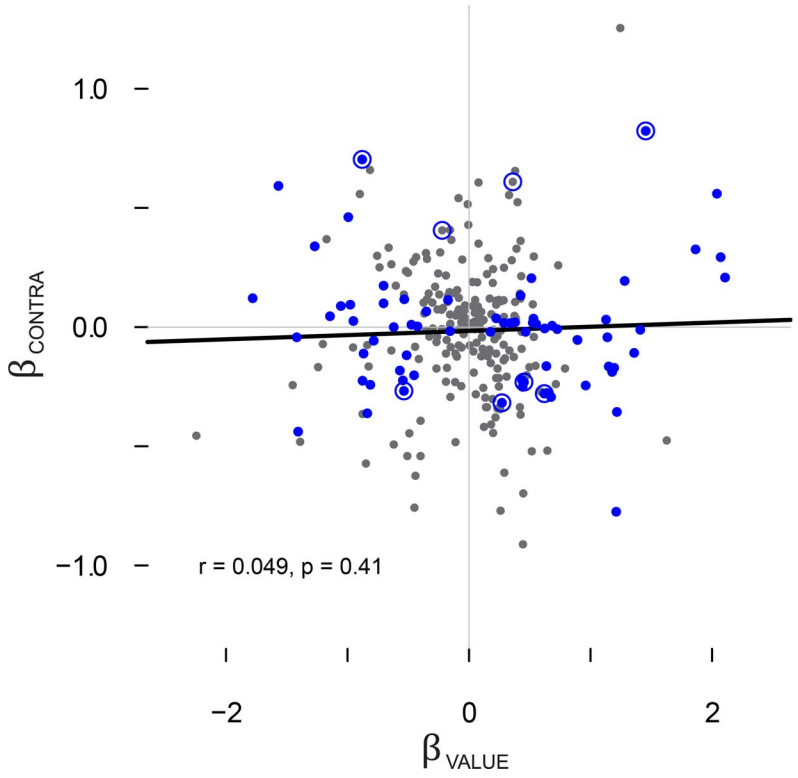

Figure S6, related to Figure 5: value preference compared to preference to contralateral cues. We asked whether a cell's preference for higher- or lower-valued cues (corresponding to positive or negative values of β_{VALUE}, respectively) was correlated with a tendency to fire more or less for fixations that placed the cue in the visual hemifield contralateral to the recording site. See Peck at al. (2013), and compare to their Figure 3B. We fit a GLM that explained fixation-evoked firing as a function of two variables: cue value, and a dummy variable indicating whether, for a given fixation, the cue was placed in the hemifield contralateral to the recording site. To maximize the possibility of detecting neurons with contra/ipsilateral firing preferences, we only used fixations located greater than 5 degrees to the left or right of the cue (which excluded on-cue fixations from this analysis). The resulting regression coefficients (β_{VALUE} and β_{CONTRA}) are compared in the scatter plot above. Each cell is indicated by a point. Solid blue points indicated a significant effect of β_{VALUE} ($p<0.05$, corrected), and blue ring, a significant effect of β_{CONTRA} ($p<0.05$, corrected). Unlike in the amygdala recordings reported by Peck et al. (2013), there is no correlation between these effects. The solid black fit line and statistics refer to Pearson's correlation coefficient. Using Spearman's coefficient, the correlation is rho = -0.080 and p = 0.18).

TABLE S1, ADDITIONAL GLM RESULTS

% of neurons with effects at p<0.05 corrected	Regressors		
	value	distance	value-by-dist
Monkey 1 (n=144)	41.7	43.0	9.7
Monkey 2 (n=139)	30.2*	18.0*	7.9
single unit (n=176)	36.4	31.2	8.5
multi-unit (n=107)	35.5	29.9	9.3
using same firing window for all cells	36.9	30.5	11.7

Table S1, related to Table 1: The percentage of neurons with significant effects in the primary GLM (Equation 1). * indicates significant difference from Monkey 1 ($p<0.05$ by chi-squared test for proportions). To generate the results in the bottom row, spiking was measured using the same 200ms post-fixation firing window in all cells (160-360ms, center at 260ms), which was the median window across all the cell-specific windows used in the main analysis.

SUPPLEMENTAL EXPERIMENTAL PROCEDURES

Subjects and apparatus

All procedures were performed in accordance with the NIH Guide for the Care and Use of Laboratory Animals, and were approved by the Animal Care and Use Committee of Stanford University.

The subjects were two adult male rhesus monkeys (13.5-15.0 kg) designated Monkey 1 and Monkey 2. Using aseptic surgical techniques, they were implanted with an MR-compatible head holder; later, a craniotomy was performed allowing access to the right OFC in Monkey 1 and left OFC in Monkey 2, and a recording chamber (Crist Instruments, Hagerstown, MD) was implanted over the craniotomy. The monkeys performed the behavioral task while head-restrained and seated ~57 cm from a fronto-parallel CRT monitor used to display the task stimuli (background luminance ~4 cd/m^2). Eye position was monitored at 400Hz using a scleral search coil system (C-N-C Engineering) in Monkey 1, and a non-invasive optical system in Monkey 2 (Eyelink, SR Research). These different eye tracking methods yield similar data (Kimmel et al., 2012).

A tube for fluid rewards was placed ~2-4mm outside the mouth, and the monkeys could only obtain all of a given reward by touching their tongue to the end of the tube during delivery. Both monkeys quickly learned to retrieve the juice in this way, and typically consumed all of the juice delivered on every trial.

Contact between the tongue and juice tube (the “licking response”) was detected by connecting the input lead of a single channel amplifier (A-M Systems, 400Hz sampling) to the fluid reservoir, and the ground to the seat of the primate chair. Tongue contact abruptly reduced the amplitude of ambient (e.g. 60Hz) noise on the channel, so that the presence/absence of contact could be determined by setting an appropriate noise threshold for each session. The licking-vs.-time plots in Figure 1 and Figure S3 show the percentage of trials in which contact was present at a given time point.

Task flow and stimulus presentation were controlled using the REX software suite (Laboratory of Sensorimotor Research, National Eye Institute) and dedicated graphics display hardware (Cambridge Research Systems). Neural signals were measured from single tungsten electrodes (FHC Inc., Bowdoin, ME) placed at the target

locations using a motorized drive (NAN Instruments, Nazareth, Israel). Neural activity, eye position, and task event data were acquired and stored using a Plexon MAP system (Plexon, Inc., Dallas, TX).

Behavioral task

In every session the subjects performed a behavioral task in two separate parts: an initial conditioning phase, in which subjects learned arbitrary cue-reward associations, and subsequent neural recording phase, in which we measured OFC activity during task performance.

In this task, we used a form of Pavlovian conditioning (Morrison and Salzman, 2009) to train the monkeys to associate three different color cues with the delivery of three juice volumes: ~3 drops (large reward), 1 drop (small reward), and 0 drops (no reward). We used a ~3:1:0 ratio to elicit three distinct levels of behavioral response in the subjects (licking, see Figure 1B). The juice volumes were constant within a session, but the ratio of large to small reward volume varied across sessions (2.5-2.7 for Monkey 1, and 2.5-3.0 for Monkey 2), to compensate for small changes in the subjects' fluid sensitivity across the duration of the study.

The trial structure in both phases was identical, and illustrated in Figure 1A. Trials began with the presentation a gray square fixation point (FP, 0.5 degrees per side), placed randomly 5 degrees to the left or right of the screen center. After the FP was fixated for a randomly chosen interval of 1-1.5 seconds, one of the three color cues was selected at random and presented at the location of the FP. The cues were square color patches, 3.2 degrees per side, and mutually equiluminant at ~22 cd/m^2. Once the cue appeared, the monkey was free to move his eyes for the duration of the trial. Gaze position was monitored while the cue was shown, but fixations had no consequence for trial outcome, which was perfectly predicted by the cue. On large and small reward trials, juice delivery began (fluid solenoid opened) exactly 4 seconds after cue onset. In all trials, the cue remained visible until about 4.3s after onset, corresponding to the end of reward delivery (solenoid closing) for the large reward cue. Trials were separated by a random 2-4 second inter-trial-interval (ITI), which lasted from the previous cue offset to the appearance of the next FP.

New cue colors were chosen at the beginning of each session (by randomly sampling equidistant points on a color wheel within the CIELUV color space), requiring the animals to learn the new color-reward associations prior to data collection. Learning was assessed each session by measuring the total duration of tongue contact with the juice tube (licking response) in the 4 second period *prior* to juice delivery (Fiorillo et al., 2008; Morrison and Salzman, 2009). This anticipatory licking was indiscriminate at the start of a new session when reward associations were unknown (not shown), and then with subsequent trials became commensurate with the reward size: large > small > no reward, with no reward ≈ 0 seconds. The initial conditioning phase was terminated when licking durations over the prior 60-100 trials were significantly different for all three trial types (rank sum test, $p<0.01$ uncorrected). See Figure 1B for average licking after initial conditioning was complete.

After the termination of the conditioning phase, the subjects continued to perform the task while we isolated and recorded suitable neural activity (see below). Thus, neural data was collected only *after* the cue-reward pairings had stabilized.

During some neural recordings, we executed a “reversal test”, in which the cue-reward associations of the no-reward and large reward cues were switched abruptly and without warning (Morrison and Salzman, 2009; Thorpe et al., 1983). The monkeys typically learned the new associations within 5-10 presentations of each cue, which we confirmed by assessing post-reversal licking behavior with a rank sum test, as was done for the initial cue-reward conditioning. Reversals occurred only during the neural recording phase, typically after data had been obtained for 300-600 trials under the initial cue-reward associations. By recording neural responses both before and after reversal, we were able to assess the effects of cue color (independent of value) on OFC neural activity.

With the exception of the reversal test, we took several steps to ensure that subjective cue value remained stationary over the period during which neural data were collected and analyzed. First, when a reversal was performed, the first 40 trials after reversal were not used for neural data analysis, which was sufficient time for the new cue-reward associations to be learned, and for OFC responses to adapt (Morrison et al., 2011). Second, all analyses except those for Figure S3 (which focuses on the effects of

reversal) use *only* either pre- or post-reversal data for a given cell, but never both, based on which block contained the most trials. Third, a session was discarded if the licking responses did not maintain selectivity after data collection began; these sessions were rare. Thus, the main analyses of this paper use data in which cue-reward associations were well learned and did not change within the experimental session.

Recording and data collection

We recorded from 283 neural unit signals in OFC, 144 from Monkey 1 and 139 from Monkey 2. Single electrodes were introduced into the brain through a sharpened guide tube whose tip was inserted 1-3mm below the dura. OFC was identified on the basis of gray/white matter transitions, and by consulting a high-resolution MRI acquired from each animal after chamber implantation. We targeted the fundus and lateral bank of the medial orbital sulcus and the laterally adjacent gyrus (Figure 1C,D), a region targeted in several other studies (Morrison and Salzman, 2009; Padoa-Schioppa and Assad, 2006; Tremblay and Schultz, 1999; Wallis and Miller, 2003), corresponding approximately to Walker's area 13 (Öngür and Price, 2000).

We typically used two electrodes simultaneously at different sites within the OFC. After initial conditioning (and while subjects continued to perform the task) we searched for neural signals using the following protocol: First, we slowly advanced the electrodes through the OFC until we isolated putative "single units", indicated by large and well-isolated waveforms, on both electrodes. Next, we collected data for 40-60 pilot trials, and used them to generate peristimulus firing rate histograms (PSTHs) of firing time-locked to cue onset, averaged across all trial types (cue values). Based on visual inspection of the PSTHs, we determined whether any of the single units showed "task-related firing", broadly defined as any apparent increase, decrease, or other change in firing rate at any point during the 0-4s cue display period. Because the PSTHs were averaged across trial types, they did not show whether cells encoded cue value, and so value encoding was not a criterion used to assess task-related firing. Likewise, fixation data were not used or referenced when constructing these PSTHs, so gaze encoding was not a criterion used to assess task-related firing. If any single unit on either electrode showed apparent task-related firing, data collection began for both electrodes.

(Thus, not all single units in the data set showed task related firing.) Otherwise, the units were abandoned, and the search continued. The process was repeated until at least one task-responsive single unit was found.

Importantly, in addition to single unit signals, we also collected any "multi-unit" signals (low amplitude, poorly isolated waveforms) that were present at the same time. Note that multiunit signals were *not* subject to the online screening described above: if they were present at the time data collection began, they were recorded regardless of their task-related activity, and then analyzed alongside the single units. As a result, this data set contains single units that were screened for task-related activity according to the broad criteria above, as well as unscreened multi-unit signals.

To avoid confusion, we use the terms "single unit" or "multi-unit" when referring to individual responses (as appropriate), and the terms "cells" and "neurons" when referring to group data that encompasses both single and multi-unit responses.

After data collection, spikes were assigned offline to individual units based upon the principal component features of the waveforms (Plexon Offline Sorter 2.0). On rare occasions, neurons initially designated as single units were re-categorized as multi-unit signals, if they showed an abundance of short inter-spike intervals (more than 0.05% of intervals below 2ms). After offline spike sorting, 176 neurons were designated as single units, and 107 as multi-unit. Our findings do not differ between single- and multi-unit signals (Table S1), and so they are presented together. After unit sorting, the data were imported into MATLAB and the R software environment for analysis.

Data Analysis

Overview The objective was to determine how neural activity was modulated by both cue value and by the location of fixation. Because the subjects were free viewing, fixation timing and location were highly variable across trials; thus, the fundamental units of analysis were individual fixations, not individual trials.

First, from the eye position data we detected individual fixations (periods of stationary gaze), and counted the spikes in a 200ms window following fixation onset (see below). We call these spike counts the "fixation-evoked firing" or "fixation-evoked response" (Figure S1), and they served as the fundamental unit of observation for most

analyses. We then used generalized linear models (GLM's) to quantify the effect of cue value and gaze location on each cell's firing. For some analyses, we fit GLM's to data in which the fixation-evoked firing rates were randomly permuted across the observations, in order to test null hypothesis that firing was random with respect to the independent variables.

Unless otherwise specified, to test for differences in means, we used Wilcoxon rank sum tests, which are robust to outliers and non-normally distributed data. Correlations were assessed using Spearman's *rho*, an outlier-resistant measure of association. When p-value corrections were applied, Holm's modification of the Bonferroni correction was used with a threshold of $p<0.05$.

Fixation detection, data selection, and extraction of fixation-evoked firing. The basic unit of analysis was an individual fixation, given by a period of stable gaze bracketed by saccadic eye movements. Saccades and fixation epochs were detected using methods described by Kimmel et al. (2012), based upon the work of Engbert and Kliegl (2003). Briefly, in each trial we calculated the variance of the horizontal and vertical components of eye velocity within that trial; we then established a velocity threshold that was defined as the ellipse whose radii were 6 times the horizontal and vertical variances. Saccades were defined as epochs >5ms in which velocity exceeded the threshold ellipse, and fixations were defined as the epochs of stable gaze between saccades. Fixation onset was defined as the first time-stamp at which the velocity decreased to within the threshold ellipse, unless the saccade appeared to slightly overshoot the cue location (occurring in 51.1% of fixations used for analysis), in which case fixation onset was the point of maximal overshoot – i.e. the beginning of the first "ring" phase, described in detail in Kimmel et al. (2012).

This procedure allowed us to compute a key variable: the *time of onset of each fixation*, which we used to determine which fixations were eligible for analysis, and as a reference time for measuring fixation-associated firing (details below, see also Figure S1). For a fixation to be eligible for analysis, it had to meet three criteria. First, its *onset* had to occur between t=0.5 and 3.75 seconds after cue onset, to exclude from analysis any firing related to cue onset or reward delivery (at t=0 and 4 seconds, respectively).

Note that this explicitly *excludes* fixations that begin before t=0.5s but continue beyond this time. Second, the fixation location had to be within 24 degrees of the cue center, and the preceding saccade amplitude had to be < 35 degrees, to stay within the calibrated range of the eye tracker. Third, fixation duration had to exceed 100ms. This, combined with the time necessary to perform a saccade (mean ~60ms), allowed for consecutive fixation onsets to be separated in time, so that spiking associated with two consecutive fixations could be distinguished from one another.

To simplify the analyses, we focused on firing *after* the onset of each fixation. This is justified by the fact that OFC neurons typically respond to visual stimuli at a latency of 100ms or more (presumably due to obligatory visual processing (Kravitz et al., 2013)), and is similar to the approach used by others to assess ventral visual stream neural activity during free viewing (DiCarlo and Maunsell, 2000; Sheinberg and Logothetis, 2001).

In particular, for each fixation we computed the fixation-evoked firing, illustrated in Figure S1, which was the spike count within a 200ms window following the onset of each fixation. Importantly, the start and end of the post-fixation time window was defined uniquely for each neuron, to account for cells that have different response latencies to changes in visual input. The time window was defined as follows: We collapsed across all trial types (cue values), and identified fixations onto the cue (< 3 degrees from center) that were immediately preceded by fixations away from the cue (> 3.5 degrees). These instances were chosen in order to capture at a coarse level how a cell responds to an abrupt change in visual input – i.e. moving gaze from a non-cue location onto the cue. We then constructed a PSTH aligned to the onset of these on-cue fixations (10ms resolution), and measured average spiking from 0 to 600ms after fixation onset. Within this range, we then searched for the 200ms window with the greatest change in firing rate (*increase or decrease*) relative to the average firing over the 1500ms preceding fixation onset – a long "baseline" interval that by design averages over many prior fixations. Thus, the earliest possible window began at 0ms and ended at 200ms after fixation, and the latest possible window began at 400ms and ended at 600ms. The median analysis window across all cells began at 160ms and ended at 360ms.

The primary analyses in this paper use the cell-specific firing windows as described above. However, we also performed some analyses using a fixed post-fixation window for all cells (Table S1), or using all time windows from 0 to 600ms (Figure S2).

Because the firing window was 200ms in duration, it was possible for a single spike to be counted as being evoked by *two* fixations, if they began within 200ms of one another. However, fewer than 4% of fixations had the potential to produce twice-counted spikes, due, primarily, to the sparse firing of many neurons, and the fact that fixation onsets were separated in time by a 100ms minimum dwell duration (above) plus the time needed for the intervening saccade (~60ms on average). Separate analyses that excluded these fixations (not shown) yielded results that were virtually the same as those shown here.

Spiking data was not normalized or smoothed, except in Figure 5D-K, where the spike counts were scaled within each neuron to between 0 and 100%, measured across all fixations.

Main General Linear Model. Our main results are based on the estimation of the following GLMs, which assumed that fixation-evoked spike counts follow a negative binomial distribution. This is a count-based distribution for which the variance is equal to or greater than the mean (McGinty et al., 2013; Venables and Ripley, 2002), which is often the case in cortical neurons (Ardid et al., 2015; Churchland et al., 2010). Although the neural responses to value and gaze distance were not linear in all cells, preliminary inspection of the data indicated that treating them as linear was a good approximation for most neurons.

The specification of the main GLM is given by

$$\log(Y) = \beta_0 + \beta_{VAL} * Value + \beta_{DIST} * Distance + \beta_{VALxDIST} * Val \times Distance \quad (1)$$

where each observation is a fixation (as defined above), *Y* is the fixation-evoked firing for that fixation, *Value* refers to the volume of juice associated with the cue in each trial (scaled so that 0 corresponds to the no-reward cue and 1 corresponds to the large cue),

Distance refers to the distance of gaze from the cue center for each fixation (coded in degrees; range 0 to 24), and *Val × Dist* is the interaction of the Value and Distance variables (computed after centering them).

Note that this model codes fixation location as a single variable: the angular distance of fixation from the cue. As described below, we carried out additional analyses to test for other spatial representation schemes (see below).

The GLMs were estimated for each neuron separately. We then carried out population-level comparisons using a variety of tests. Unless otherwise specified, to test for differences in means, we used Wilcoxon rank sum tests, which are robust to outliers and non-normally distributed data. Correlations were assessed using Spearman's *rho*, an outlier-resistant measure of association. When p-value corrections were applied, Holm's modification of the Bonferroni correction was used with a threshold of $p<0.05$.

Alternative GLMs. We estimated two additional GLMs to assess the plausibility of alternative schemes for encoding fixation location. The first one used the absolute angle of gaze in head-centered coordinates, which leads to the following specification:

$$\log(Y) = \beta_0 + \beta_{VAL} * Value + \beta_{ANG} * Angle + \beta_{VALxANG} * Val \times Angle. \quad (2)$$

The second used horizontal and vertical distances to the cue, which leads to the following specification:

$$\log(Y) = \beta_0 + \beta_{VAL} * Value + \beta_{HOR} * Horizontal + \beta_{VER} * Vertical\ . \quad (3)$$

The relative fit of the models was evaluated by comparing the goodness of fit for each alternative model to the one for the main model, using Akaike's information criterion (AIC).

Comparison of initial cue-evoked value signal with value signal during free viewing

Results in main text. Firing was measured 50-500ms after cue onset, and a GLM was fit in which this firing was explained by a single regressor: cue value. To assess value

coding during the cue viewing period (0.5-3.75s), a GLM was fit explaining fixation-evoked firing as a function of cue value, using *only* the fixations <3 degrees from the cue. These fixations were used, because, at onset, the cues were always presented at the center of the fixation window and therefore near the center of gaze; we wished to select from the cue viewing data a subset of fixations that likewise placed the cue near the gaze center. The beta coefficients for cue-evoked and fixation-evoked value encoding were compared using Spearman's correlation coefficient.

GLM for color/value reversal test Results in Figure S3. For the GLM applied to the reversal test data, the three regressors were cue *Value*, the cue *Color* (coded as a two-level factor), and the *Value-by-Color* interaction. Significance was assessed at the $p<0.05$ level, corrected.

GLM with oculomotor co-regressors Results in Figure S4A-B. We asked whether the GLM results shown in Table 1 and Figure 5 could be explained by oculomotor variables other than the distance of fixation from the cue. For each cell we fit a GLM using the same terms as Equation 1, but with three additional regressors that describe other oculomotor features: the amplitude of the saccade prior to the fixation, the velocity of that saccade, and the dwell time of the fixation. The percentage of significant effects were calculated in the same manner as for Table 1.

Effects of fixation dwell time and saccade amplitude on fixation-evoked excitation Results in Figure S4C-D. The GLM with oculomotor co-regressors described above indicated that very few neurons significantly encoded fixation dwell time or amplitude of the preceding saccade, suggesting that these two oculomotor variables contribute only negligibly to fixation-evoked firing. To confirm this, we selected a subset of the data designed to hold the cue value and fixation location constant, and asked whether fixation-evoked firing was modulated by either dwell time or saccade amplitude. The data subset was constructed as follows: First, only fixations onto the cues were used (distance < 3 degrees); these were chosen because they are the most frequently visited single location (Figure 2). Second, the data were restricted to isolate only neurons with

excitatory responses to on-cue fixations (effect of β_{DIST} $p<0.01$, uncorrected), because they were more prevalent than neurons inhibited by on-cue fixations (Figure 5B, D). Third, within each cell, only the trial type (cue value) that produced the largest fixation-evoked excitation was used, in order to keep cue value constant. This resulted in a subset of 69 neurons with sufficient data for analysis.

Thus, by design, the average fixation-evoked response in this data subset was excitatory; the question we asked is how this excitation is modulated by dwell time and saccade amplitude. To assess saccade amplitude effects (results in Figure S4D), the fixations for each were cell were divided according to whether the prior fixation was near the cue (< 3 deg., blue) or away from the cue (> 10 deg., black, n=69); because all fixations in the subset were < 3 degrees from the cue, dividing by prior location in this way effectively divides them according to saccade amplitude. To assess the dwell time effects (results in Figure S4C), the data subset was further refined to include only fixations that were immediately preceded *and followed* by fixations away from the target (yielding 59 neurons with sufficient data), so that consecutive fixations onto the cue were excluded. Then, for each cell, the fixations were median split into those with "short" and "long" dwell times, and the average responses were plotted in PSTHs.

Permutation tests. For some GLMs, we address the issue of multiple comparisons by fitting the GLMs to data for which the spike counts were permuted. Permutation was performed by randomly shuffling the fixation-evoked spike counts among the fixations within a given cell, eliminating any systematic relationship between spiking and the regressor variables, leaving only chance correlations. We thereby establish the "chance levels" of the statistics shown in Table 1, with the following procedure: First, we created 1000 permuted data sets by randomly shuffling the spikes in every cell in the population 1000 times. We then fit GLMs to the permuted cells. Then, for each variable of interest, we calculated the percentage of significant effects (which are spurious by due to the permutation) in each of the 1000 sets; the maximum percentage across all sets was taken to be the maximum expected by chance. This provides a very conservative estimate of the different statistics that could be observed by chance, and leads to a confidence level equivalent to $p<0.001$.

Responses to the FP We also examined firing evoked by the onset of the fixation point (FP) at the beginning of each trial, to test whether these responses were also modulated by the distance of fixation from the stimulus. For this data, we estimated a GLM that contained only a single regressor: the distance of gaze from the FP at the time of onset. The resulting estimates of $\beta_{DIST\text{-}FP}$ were then compared to the estimates of β_{DIST} described above (Main GLM, Equation 1), on a cell-by-cell basis.

We measured firing time-locked to each FP onset by counting the spikes within the same cell-specific 200ms windows described above. Analysis was restricted to include FP onsets for which the gaze was < 24 degrees from the FP (matching the range for fixations in the value cue data), was stationary at FP onset, and remained stationary for at least 100ms thereafter (matching the minimum fixation dwell time in the value cue data). We required at least 50 such acceptable FP onsets for each cell, the minimum necessary to fit the GLM. This yielded 228/283 cells eligible for this analysis. The resulting estimates of $\beta_{DIST\text{-}FP}$ were compared to the β_{DIST} using Spearman's correlation coefficient.

To interpret the resulting correlation, we asked whether the observed correlation between β_{DIST} and $\beta_{DIST\text{-}FP}$ is subject to an upper bound due to noisiness inherent in their estimation, or to the fact that fixation locations in the value cue data differed from fixation locations at FP onset. To estimate this upper bound, we calculated the reliability of each data set (R_{DIST}, R_{FP}) using a split halves procedure and Spearman-Brown correction. Assuming that the underlying effects are identical in the two contexts, the upper limit for the correlation is given by the square root of R_{DIST}*R_{FP} (See Supplemental Experimental Procedures and Nunnally (1970)). As a complement to this calculation, we also used a resampling procedure to assess how the β_{DIST} for the value cue data would correlate with *itself,* but under sampling conditions that that closely approximated the ones used to estimate $\beta_{DIST\text{-}FP}$, in terms of number of observations and the distribution of gaze distances (see Supplemental Experimental Procedures).

Finding the upper limit on the correlation between gaze effects in Figure 6C Results in main text. We used two methods to estimate the theoretical upper limit on the

correlation between β_{DIST} and $\beta_{DIST\text{-}FP}$ (reported in Figure 6C), a limit that results from the inherent noisiness of the two sets of coefficients, as well as differences in the sampling of visual space in the FP onset and cue viewing contexts. Both methods used the value cue data in Figure 5, and the FP onset data set described in the main text.

Method 1, reliability statistics**:** To estimate the reliability of β_{DIST}, we use the "split-halves" procedure: the data in each neuron are split into even and odd trials, and the main GLM (Equation 1) is run on each half of the data (Nunnally, 1970). This yields two sets of beta values, and we find the Spearman's correlation (*rho*) between these two halves. We then apply the Spearman-Brown correction to this statistic:

$$\frac{n * rho}{(1 + (n - 1) * rho)}$$

using $n = 2$ to scale to the full size of the data (Nunnally, 1970). This gives the expected *reliability* (R_{DIST}) of the full data set, i.e. the correlation that could be expected between the existing data, and a new data set of the same size (same number of trials per cell) collected from the same cells. Using the same procedure, we find the reliability of the distance beta coefficients in the FP onset data (R_{FP}).

Given the reliability statistics from two data sets *A* and *B*, one can find the theoretical maximum correlation that could be expected between *A* and *B.* This is given by:

$$\bar{r}_{AB} * \sqrt{R_A * R_B}$$

where R_A and R_B are the respective reliabilities of *A* and *B*, and $\bar{r}_{AB}$ is the true correlation of the *underlying effects* that generate *A* and *B* (Nunnally, 1970). If we assume that the effects in A and B are identical, then $\bar{r}_{AB}$ is equal to 1, and the maximum observed correlation in the data is the square root of the product of the reliabilities.

Method 2, resampling: Resampling proceeded as follows: for a given cell, the data in both sets were divided according to the fixation distance from the cue/FP, into 0.5 degree bins. Then, for each bin, samples were drawn *with replacement* from the

value cue data, until the number of samples was equal to the number of observations in that particular distance bin in the *FP data*. The proportion of no reward, small reward, and large reward cues approximated the proportion in the original value cue data.

A GLM (Equation 1) was then fit to these resampled value cue data, and the resulting β_{DIST} was compared to the original β_{DIST} (from Figure 5) at the population level using Spearman's correlation coefficient. This resampling, estimation, and correlation was performed 500 times to produce a distribution of correlations between the original and resampled data. (Resampled data sets differ from one another because sampling is performed with replacement.) We then interpreted the resulting correlations as the practical upper bound for the correlation that could possibly be observed between the β_{DIST} estimates obtained from the value cue and FP data sets.

Because the resampling was performed with replacement using discrete gaze distance bins, even a data set that is resampled to match the original (at a precision of 0.5 degrees) would likely have a correlation with the original data of < 1.0, implying that this method itself imposes an upper limit to the self-similarity that can be measured in our data. To estimate this limit, we performed the above procedure (500 replications) on value cue data resampled to match *its own* number of observations and gaze distance distribution. The median self-correlation was *rho* = 0.928, with 99% of observations between 0.895 and 0.953. The fact that this correlation is < 1.0 means that the resampling procedure itself introduces an artefactual "loss" of self-correlation, even when the resampling attempts to match the original. However, this degree of artefactual loss is small compared to the decrease in self-correlation that results when the value cue data were sampled to match the FP data (see text).

SUPPLEMENTAL REFERENCES

Bruce, C.J., Goldberg, M.E., 1985. Primate frontal eye fields. I. Single neurons discharging before saccades. J. Neurophysiol. 53, 603–635.

Engbert, R., Kliegl, R., 2003. Microsaccades uncover the orientation of covert attention. Vision Res. 43, 1035–1045. doi:10.1016/S0042-6989(03)00084-1

Kimmel, D.L., Mammo, D., Newsome, W.T., 2012. Tracking the eye non-invasively: simultaneous comparison of the scleral search coil and optical tracking techniques in the macaque monkey. Front. Behav. Neurosci. 6, 49. doi:10.3389/fnbeh.2012.00049

Nunnally, J.C., 1970. Introduction to Psychological Measurement. McGraw-Hill Book Company.

Sheinberg, D.L., Logothetis, N.K., 2001. Noticing Familiar Objects in Real World Scenes: The Role of Temporal Cortical Neurons in Natural Vision. J. Neurosci. 21, 1340–1350.